Tidal influence on soil conditions in an intertidal creek-marsh system

Pei Xin[1,#], Ling Li[1,2], and D. A. Barry[3]

[1] National Centre for Groundwater Research and Training, School of Civil Engineering, The University of Queensland, Queensland, Australia

Emails: p.xin@uq.edu.au, l.li@uq.edu.au

[2] State Key Laboratory of Hydrology-Water Resources and Hydraulic Engineering, Ho-hai University, Nanjing, China

[3] Laboratoire de technologie écologique, Institut d'ingénierie de l'environnement, Faculté de l'environnement naturel, architectural et construit (ENAC), Ecole Polytechnique Fédérale de Lausanne (EPFL), Station 2, 1015, Lausanne, Switzerland

Email: andrew.barry@epfl.ch

***Water Resources Research,* accepted on November 29, 2012**

[#] Author to whom all correspondence should be addressed. Tel: +61 7 33469820

Abstract

To understand better how tides affect the soil conditions of salt marshes, pore-water flow in a modeled 3-D creek-marsh system was simulated under the influence of both monochromatic and spring-neap tides. In analyzing the simulation results, we examined six indices, viz., marsh surface elevation, hydroperiod, shortest distance to creeks, mean soil water saturation, soil saturation index and net water flux across the marsh surface. The results demonstrated that mean soil water saturation, soil saturation index and net water flux exhibited corresponding patterns of spatial variations, which were related to marsh surface elevation, hydroperiod, shortest distance to creeks and tidal regime. While the relationships could be described by a simple function under monochromatic tides, under spring-neap tides it was more complex with different behaviors in the lower and upper marsh areas. The shortest distance to creeks was a critically important factor affecting soil conditions. Well aerated and drained zones co-existed near the creek under both monochromatic and spring-neap tides. Spring-neap tides led to improved soil aeration in the upper marsh, including the interior section (away from the creek) where the hydroperiod and inundation frequency were reduced during neap tides. However, the local flushing condition did not improve correspondingly. The study suggests that single morphological index cannot describe the soil conditions adequately. A proper representation of the soil conditions for plant growth and distribution should take into account not only the aeration condition but also the flushing condition. For that purpose, a composite index is needed to combine the soil water saturation index and the net flux index.

Key words: Salt marsh, Pore-water flow, Soil aeration, Flushing, Plant growth, Salinity stress

Key Points:

- Six indices describing the soil conditions in salt marshes were studied
- Effects of monochromatic and spring-neap tides were examined
- Marsh morphology and tidal regime jointly affect the soil conditions

1. Introduction

Salt marshes are intertidal wetlands vegetated by herbs, grasses and low shrubs [*Chapman*, 1960; *Armstrong*, 1982; *Vernberg*, 1993]. Plants in these wetlands are commonly found to be organized in spatial patterns, i.e., plant zonation [*Chapman*, 1960; *Marani et al*., 2006; *Sadro et al*., 2007]. Many studies have been conducted to examine how the plant growth and distribution are affected by various factors, including marsh morphology, soil properties, species competition, surface water hydrodynamics and subsurface flow processes [*Vernberg*,1993; *Silvestri et al*., 2005]. Ecologists, particularly, have paid attention to marsh morphology.

It has been suggested that oxygen availability in the marsh soil, affecting plant root respiration, plays an important role in governing the plant growth [*Dacey and Howes*, 1984; *Colmer and Flowers*, 2008]. Since the oxygen diffusivity and concentration in pore-water are much lower than those in the air [*Armstrong and Drew*, 2002], oxygen availability is determined predominantly by the soil aeration. Salt marshes are periodically inundated by the tidal water, which can lead to poor aeration with oxygen depleted in the marsh soil, adversely affecting the plant growth [*Dacey and Howes*, 1984; *Ursino et al*., 2004; *Li et al*., 2005; *Marani et al*., 2006]. Attempts have been made to establish relationships among the soil aeration, spatial plant distribution and marsh morphology as well as other factors (e.g., *Silvestri et al*. [2005]; *Moffett et al*. [2010]). A number of indices have been developed to describe such relationships:

(1) Marsh **surface elevation** (SE), reflecting directly the marsh topography, is a tradi-

tional index for studying plant zonation in a salt marsh. In nature, the marsh platform typically inclines towards the coastal sea, with the maximum elevation occurring at the inland side. Different areas of the salt marsh are subjected to different degrees of inundation as the coastal water level rises and falls with the tide. Thus, the SE affects local moisture content and pore-water salinity in the soil, and hence influences the plant growth and distribution [*Silvestri et al*., 2005].

(2) **Shortest distance to creeks** (SDC) has also been adopted to study plant zonation since the creek network is a key element of marsh morphology [*Sanderson et al*., 2001; *Silvestri et al*., 2005; *Moffett et al*., 2010]. Creeks play an important role not only for transmitting tidal signals, but also for chemical (e.g., salt) transport between the marsh and coastal sea. Recent research has revealed near-creek circulating flow with surface water infiltrating the soil through the marsh platform and pore-water seeping out of marsh sediments across the creek bank and bottom [*Ursino et al*., 2004; *Gardner*, 2005; *Li et al*., 2005; *Marani et al*., 2006; *Wilson and Gardner*, 2006; *Xin et al*., 2009, 2011]. As a result, the near-creek area tends to be well aerated (for plant root respiration) and flushed (preventing overly high salinities), and hence better suited for plant growth compared with the interior area [*Mendelssohn et al*., 1981; *Howes et al*., 1981; *Howes and Goehringer*, 1994].

(3) **Hydroperiod** (HP) combines the SE and tidal fluctuations to define the regime of local inundation, i.e.,

$$\mathrm{HP} = \frac{\sum P_i}{P_T}, \tag{1}$$

where HP is the averaged hydroperiod over a reference period, P_T (e.g., period of the spring-neap tidal cycle); and P_i is the i^{th} inundation period over P_T. This is a simple yet widely used index for characterizing soil conditions [*Silvestri et al*., 2005].

The above three indices do not directly account for pore-water flow effects. In the following, we discuss three additional indices that consider them.

(4) **Mean soil water saturation** (MSS) in the root zone is the complement to that zone's average air content, and thus it can represent the soil aeration. The root zone, within the intertidal range, responds to tides with temporarily varying soil water saturation [*Xin et al*., 2009]. Measurement of the soil water saturation is non-trivial and is not carried out routinely.

(5) **Soil saturation index** (SSI) is defined as the ratio of the period of saturation to a reference period at the soil depth of the root zone [*Xin et al*., 2010], i.e.,

$$\mathrm{SSI} = \frac{\sum_{i=1}^{m} \xi \Delta t}{P_T}, \tag{2}$$

where ξ = 0 if the local groundwater table is below the root zone; otherwise ξ = 1; Δt is the incremental period (e.g., time step used in the simulation) and m is the total number of incremental periods over the whole reference period (P_T). SSI varies between 0 and 1, representing respectively the permanently aerated and non-aerated conditions over P_T. Since the oxygen diffusivity and concentration in the pore-water are much lower than those in the air, the saturated condition (SSI = 1) can be treated as being unsuitable for plant growth. Note that the calculation of SSI is relatively simple, based on the local water table elevation.

The characterization of the soil conditions for the marsh plant growth by the above five indices is incomplete since other factors are neglected, particularly nutrient availability and salinity stress. For example, the soil salinity has been found to affect plant growth and distribution because of differences in the tolerance of plant species to salinity [*Silvestri and Marani*, 2004; *Pennings et al*., 2005]. The near-creek circulation, discussed earlier, provides a key mechanism for solute (nutrient and salt) transport in the marsh soil, affecting the soil conditions in terms of nutrient availability and salinity stress for plant growth.

(6) **Net water flux (NWF) across the marsh surface** associated with the tide-induced circulation is introduced here to represent further the soil conditions. This flux, as an indicator of the local drainage/flushing condition, is likely to correspond negatively with the soil moisture and soil salinity. Inadequate flushing may allow local pore-water salinity to increase markedly under the influence of evapotranspiration, resulting in hyper-salinity that would affect plant growth and distribution in salt marshes [*Morris*, 1995; *Silvestri et al*., 2005]. As discussed by *Xin et al*. [2011], the temporal scale of the tide-induced pore-water circulation varies by orders of magnitude within the marsh system. Direct simulations of solute transport in the marsh soil under the influence of such a flow condition would take very long time to reach a quasi-steady state (for which the solute has moved through a complete circulation cycle through the marsh). Therefore, the solute exchange between the surface water and groundwater in the modeled marsh system was not simulated directly; instead the analysis was based on the net water flux, as an indicator for the solute transport and concentration in the marsh soil.

The first three indices listed above have been used widely in previous studies of plant zonation in salt marshes [*Silvestri et al*., 2005; *Moffett et al*., 2010]. The correspondence of these indices with plant distributions varied case-by-case due to the complexity of natural marshes. With the effect of pore-water flow incorporated, the last three indices are expected to correlate better with the plant growth and distribution. Using SSI, *Xin et al*. [2010] conducted numerical simulations to identify two characteristic zones of soil aeration over a cross-creek section subjected to the influence of spring-neap tides: a relatively well aerated near-creek zone and a poorly aerated interior zone, a result consistent with field observations of plant zonation along the creek [*Mendelssohn et al*., 1981; *Howes et al*., 1981; *Howes and Goehringer*, 1994]. By contrast, the hydroperiod would indicate an unrealistic, uniform soil inundation (aeration) condition across the section. While the work of *Xin et al*. [2010] highlighted the effect of spring-neap tides on soil conditions, it was based on a cross-creek section rather than a more realistic, 3-D marsh system.

Recently, *Xin et al*. [2011] presented a modeling study of a synthetic 3-D creek-marsh system and revealed multiscale pore-water flows in the form of near-creek circulation, meander-modulated circulation and near-channel circulation. These circulations are likely to be a key process underlying the variations of soil conditions in the marsh system. *Moffett et al*. [2012] simulated a 3-D marsh system based on field measurements and demonstrated complex spatial variations of soil conditions. This work revealed important interplays of multiple factors (including soil heterogeneity, topography, vegetation, groundwater and surface water dynamics) in affecting the eco-hydrological zonation of the marsh system, motivating further research to examine the details of underlying mechanisms.

The present study aims to explore the link between pore-water flows and soil conditions in a 3-D salt marsh subjected to the influence of spring-neap tides. Spring-neap tides commonly occur at natural coasts [*McKee and Patrick*, 1988; *Chen*, 1998; *Montalto et al*., 2006], with the tidal range varying from the maximum at the spring tide to the minimum at the neap tide. The variation of the tidal range results in varying extents of inundation over the marsh during the spring-neap tidal cycle – an aspect that is fundamentally different from commonly studied monochromatic systems. Based on a 3-D creek-marsh system with a layered soil configuration (a mud layer overlaying a sandy-loam layer), we simulated the pore-water flow in the marsh subjected to the influence of monochromatic (semi-diurnal) and spring-neap tides, respectively. In analyzing the effects of spring-neap tides on the behavior of the marsh compared with those of monochromatic tides, we focused on the variations of the six indices, in particular, how they combine to reflect the soil conditions in the marsh.

2. Conceptual and mathematical models

2.1. Physical conditions

The synthetic marsh examined here is similar to the base case in *Xin et al*. [2012] (Figure 1). The simulated creek-marsh system captures the characteristics of upper sections of tidal flats [*Allen*, 2000; *Novakowski et al*., 2004; *Torres and Styles*, 2007]. A meandering creek is embedded in the marsh sediment and linked to the tidally fluctuating coastal water through a main channel on the marsh edge (Figure 1). The synthetic creek-marsh system was characterized by topographic (slope) changes over three different scales: (1) large slope changes at the creek and main channel bank (0.2 and 0.1, respectively), (2) marsh surface el-

evation changes associated with the creek meander (with an maximum channel curvature of $\pi^2/500$ m^{-1}), and (3) a small uniform inclination angle (0.005 in elevation gradient) of the whole marsh platform (Figure 1, see *Xin et al*. [2011, 2012] for details).

As soil strata are commonly found in natural marshes [*Harvey et al*., 1987; *Dolphin et al*., 1995; *Hughes et al*., 1998; *Gardner and Porter*, 2001; *Perillo et al*., 2005; *Xin et al*., 2009; *Carol et al.*, 2011; *Wilson and Morris*, 2012], we generated a two-layer soil configuration with an upper low-permeability mud layer and a lower high-permeability sandy-loam layer. For the purpose of simplicity, we set the interface between the two soil layers locally at a depth (from the marsh platform) equivalent to 10% of the local sediment thickness (Figure 1). As the elevation of the marsh platform varies from 6 (marsh edge) to 7.25 m (marsh upper end), this interface varies in depth from 0.6 to 0.725 m. This stratigraphy (e.g., the thickness of a mud layer) is consistent with field observations [*Hughes et al*., 1998; *Xin et al*., 2009].

While salt marshes are also affected by evapotranspiration, precipitation and regional flow, we focused on tidal forcing in this paper. We assumed that the main channel was directly connected to tidal water and set as the coastal boundary with specified tidal level fluctuations. Two types of tidal forcing were considered:

(1) a monochromatic (semi-diurnal) tide given by (Figure 2),

$$H = Z_{\mathrm{MSL}} + A_1 \cos(\omega_1 t) \tag{3}$$

and

(2) spring-neap tides given by (Figure 2),

$$H = Z_{\mathrm{MSL}} + A_1 \cos(\omega_1 t) + A_2 \cos(\omega_2 t + \delta), \quad (4)$$

where H is the water level [L] in the main channel at the time t [T]; Z_{MSL} is the mean sea level [L]; A_1 and A_2, and ω_1 and ω_2 are the amplitudes [L] and angular frequencies [T^{-1}] of the semi-diurnal solar (S2) and lunar tide (M2), respectively; and δ is the phase difference between the two tidal constituents [-]. The bi-chromatic signals combine to produce the spring-neap tidal variations. For the semi-diurnal solar tide, T_1 = 12 h and ω_1 = 0.5236 rad/h; and T_2 = 12.42 h and ω_2 = 0.5059 rad/h for the semi-diurnal lunar tide. Thus, the spring-neap tidal cycle is formed with a longer period of $T = 2\pi/(\omega_1 - \omega_2)$ = 14.78 d [*Godin*, 1972].

2.2. Mathematical model

A coupled model based on **ELCIRC** for surface water [*Zhang et al*., 2004] and **SUTRA** for pore-water [*Voss and Provost*, 2008] was employed. The details of the coupling approach and model validation can be found in *Yuan et al*. [2011]. As we considered here silt loam, a relatively compressible soil, the compressibility of the soil matrix and water was included. To account for the effect of varying total stress on the marsh soil during the inundation, the SUTRA code was modified with a tidal loading term added to Richards' equation [*Reeves et al*., 2000; *Gardner and Wilson*, 2006; *Xin et al*., 2012]. The seepage face (with zero pressure) was allowed to develop across the marsh sediment surface. Seepage occurs across a large area of the marsh surface particularly as the tide recedes [*Xin et al*., 2011]. This circumstance clearly affects the local soil saturation, especially for low-permeability silt loam.

The model based on Richards' equation simulated the soil water saturation, the com-

plement of which within the pore space reflects the soil aeration to some extent under the assumption that air can be readily displaced by water – lower soil water saturation is related to better aeration. This is appropriate when pressure gradients in the air phase are insignificant compared with those in the water phase [*Li et al*., 2005], which we consider to be a reasonable assumption in this study. In coastal marshes, salt concentrations in surface water and pore-water can vary spatially and temporally, leading to density gradients that may affect the pore-water flow. Here, we neglected this effect by assuming a constant water density, as done in previous numerical studies [*Ursino et al*., 2004; *Wilson and Gardner*, 2006; *Xin et al*., 2009; *Xin et al*., 2011], in order to focus on effects of tides and marsh morphology in the first instance. The constant water density assumption is likely to apply to many salt marshes where freshwater input from upland is lacking.

2.3. Parameter values used in the simulations

The monochromatic tide simulations consisted of a S2 tide with an amplitude (A_1) of 1 m. For the spring-neap tides, the S2 (A_1) and M2 (A_2) amplitudes were set to 0.25 m and 0.75 m, respectively. The phase lag (δ) between the two tidal constituents was assumed to be zero. The mean sea level, Z_{MSL}, was set to 6.3 m, which allowed the whole marsh platform to be inundated at seven spring high tides over a spring-neap cycle.

Silt-loam (mud) and sandy-loam, two typical soil types commonly encountered in salt marshes, were simulated in the upper and lower layers, respectively [*Gardner and Porter*, 2001; *Schultz and Ruppel*, 2002; *Simonini and Cola,* 2002; *Cao et al*., 2012; *Wilson and Morris*, 2012]. Following *Wang et al.* [1997], the hydraulic conductivities of the upper and

lower soil layers were set to 1.25×10^{-6} m/s and 1.23×10^{-5} m/s with porosity equal to 0.45 and 0.41, respectively. For the upper soil layer, the residual water saturation, S_{Wres}, was set to 0.15, and the *van Genuchten* (1980) water retention parameters, α_v and n, to 2 m^{-1} and 1.41, respectively, according to the data for the soil type given by *Carsel and Parrish* [1988]. These parameter values would lead to a relatively thick capillary fringe with relatively high soil water saturations (> 0.9) across the whole marsh system. The lower soil layer was expected to be (near-) saturated over the tidal period. Therefore, the soil water retention parameters did not affect the flow in the lower layer. Compressibility of soil matrix and water were, respectively, set to 10^{-7} Pa^{-1} and 4.47×10^{-10} Pa^{-1} [*Freeze and Cherry*, 1979].

The initial condition, boundary conditions, time step size and mesh size were similar to those of *Xin et al*. [2012]. Time step and mesh size tests demonstrated that converged numerical results were obtained.

3. Simulation results

3.1. Groundwater table and soil water saturation dynamics

The simulated tide was uniform across the whole marsh, with the water level oscillation relative to the marsh surface elevations at various locations as shown in Figure 2. The spring tides on days 0-2 (and days 13-15) differed little from the monochromatic tide. At the spring high tide, the whole marsh was inundated. As the tide changed from spring to neap (days 3-7), the range of the water level oscillation decreased and increasingly the upper marsh area became unaffected by the tidal inundation.

In response to the spring-neap tidal oscillations, the pore-water flow and soil water saturation in the marsh varied not only between high and low tides over the semi-diurnal cycle but also between spring and neap tides over a longer period of 14.78 d. Note that a spring-neap tidal period contains around 29 semi-diurnal tidal cycles. Figure 3 shows the variations of the simulated soil water saturation near the sediment surface across the marsh at six tidal stages. At the spring high tide, complete tidal inundation of the whole marsh resulted in a fully saturated soil (Figure 3a, day 0). As the tide receded (from the high spring to low spring tide), the pore-water seeped out from the marsh soil, leading to decline of the groundwater table as shown in Figure 4 (which plots, as an example, local groundwater table fluctuations at six locations on the cross-creek section along y = 190 m). However, the decline of the water table in the marsh interior (away from the creek) was very limited with a slight drop below the local platform surface over the spring tides (days 0-4) and hence the soil remained mostly saturated in this area due to a relatively thick capillary fringe in the silt loam. Therefore, at the spring low tide aerated soil could occur only in two narrow zones near to and on both side of the creek (Figure 3b).

The poor aeration evident in the interior was improved in the upper marsh area during the neap tides. As the tidal range decreased from spring to neap tides, the extent of tidal inundation was reduced and did not reach the upper marsh area (Figure 2). A hydraulic gradient between the marsh interior and the creek (bank and bottom) persisted during this period, driving drainage to the creek [*Xin et al*., 2010]. The cumulative effect of this drainage process over the neap tides (days 5-9; Figure 4) led to a continuous decline of the local water table in the marsh interior. Across the whole marsh system, the aerated zones extended consistently

towards the marsh interior in the upper marsh area (Figures 3c-3e). However, the low-elevation marsh area was still subjected to semi-diurnal inundations with no improvement of the local soil aeration. Moreover, the low tide limit rose also as a result of the reduced tidal range. This led to shortening of the strip-like near-creek aerated zone at the lower marsh end, which developed at low tides (Figure 3c vs. Figure 3b). As the spring tides approached, the persistent drainage (with no interruption due to inundation over the semi-diurnal cycle) in the upper marsh area paused, and the whole marsh was effectively saturated due to the extensive inundation at the high tide (Figure 3f) and aerated only in the near-creek zone at the low tide.

The temporal variations of the net flux across the whole marsh surface over a spring-neap tidal cycle were examined (Figure 5a). For the simulated marsh, the flux associated with soil compressibility (with compressibility coefficient = 10^{-7} Pa^{-1}) was negligible [*Xin et al*., 2012]. Thus, the net flux was primarily related to the volumetric change of saturated pore space in the marsh soil. Overall, the rates of net influx and efflux increased with the tidal range as the tides switched from neap to spring tides. This is consistent with the findings of *Wilson and Morris* [2012]. Their 2-D model results demonstrated enhanced flushing (i.e., increased flux) of the marsh soil as the tidal amplitude increased and caused more extensive inundation of the marsh platform. The time-varying net flux was integrated from day 0 (spring high tide) to determine the cumulative flux at different times over the spring-neap cycle (Figure 5b). This cumulative flux reflects the overall degree of soil saturation in the whole creek-marsh system, i.e., a zero cumulative flux represents a fully saturated soil condition and a negative cumulative flux is related to a drained soil condition (Figure 5b).

The results showed that although both influx and efflux across the marsh surface occurred over the neap tides, the latter was dominant over each neap tidal cycle (Figure 5a). This led to an overall decrease in the cumulative flux, indicating drainage of the whole marsh system. Over the spring-neap tidal cycle, the minimum (most negative) cumulative flux occurred around day 10, approximately 2.5 d after the neap tide. This coincided with the time when the tidal level started to reach the maximum creek bank elevation (Figure 2). Afterwards, the net influx dominated over each tidal cycle and nearly the whole marsh system became saturated.

Although the tidal signal was symmetric over the spring-neap tidal cycle (Figure 2), the response of the whole marsh system to tides was asymmetrical, particularly with the minimum cumulative flux (i.e., the optimal drainage) lagging the minimum tidal range during the neap tides (Figure 5b). The delayed response, consistent with field observations [*Thibodeau et al*., 1998; *Montalto et al*., 2006; *Wilson et al*., 2011; *Cao et al*., 2012], revealed further the complexity of the marsh system in terms of dynamic, non-linear surface water and groundwater interactions. This is similar to but not exactly the same as the behavior of tide-induced groundwater table fluctuations in a coastal unconfined aquifer. These water table fluctuations exhibit asymmetry with a rapid rising phase followed by a slow falling phase over the semi-diurnal or diurnal cycles due to sub-harmonic oscillations generated by non-linear tidal wave propagation in the aquifer; however, they remain almost symmetric over the spring-neap cycle [*Li et al*., 2000; *King et al*., 2010]. In the upper part of the marsh above the neap high tide mark, the local mean groundwater table continues to decline until the inundation takes place sometime after the neap tide (Figure 2). The aggregation of such local drainage conditions leads to the overall asymmetry in the cumulative flux across the whole marsh

as shown in Figure 5b. This asymmetrical behavior suggests the presence of sub-harmonic oscillations in the marsh system over the spring-neap cycle, e.g., oscillations of period ~7.21 d for 2nd sub-harmonics.

Overall these results show that the inundation events lead to water infiltration through the soil, which affect adversely the soil aeration. On the receding tide, pore-water drainage to the creek improves the soil aeration in the near-creek area [*Ursino et al*., 2004; *Li et al*., 2005; *Marani et al*., 2006; *Xin et al*., 2009, 2011]. The results revealed further improvement of the soil aeration in the upper marsh area during neap tides. The soil water saturation exhibited interesting spatial variations associated with the dynamics of the groundwater table (Figure 3). While no field data are available for verifying these saturation variations, the simulated groundwater table behavior is consistent with field observations from previous studies (Figure 4 of *Wilson et al*. [2011]).

3.2. Spatial variations of marsh soil condition indices

Based on the simulation results, we calculated the six indices over the periods of 12 h and 14.78 d for the monochromatic and spring-neap tidal cases, respectively. Despite the same marsh morphology (Figures 6a and c vs. Figures 7a and c), the different tides led to significant differences in the spatial patterns of SSI (Figure 6d vs. Figure 7d), mean soil water saturation (Figure 6e vs. Figure 7e) and net water flux (Figure 6f vs. Figure 7f). These differences were essentially due to the changes of the inundation characteristics as indicated by the hydroperiod (Figure 6b vs. Figure 7b). As a result of the contraction of the intertidal zone during the neap tides, the hydroperiod decreased in the upper marsh area and increased in the

lower area.

Monochromatic tidal simulation

For the monochromatic tide, the marsh system exhibited two narrow strip-like zones of relatively low soil water saturation near and along the creek, as indicated by the results of SSI and mean soil water saturation (Figures 6d and 6e). Near the bank of the main channel, the soil saturation also appeared to be lower. The spatial variations (functions of x and y) of SSI and mean soil water saturation correlated highly with each other (correlation coefficient = 0.89, calculated with the "corrcoef" function in MATLAB). Given this high correlation, SSI may be preferred as an index for describing the soil saturation/aeration because its measurement based on local water table elevation is relatively easy.

Overall, the soil water saturation seemed to be related to the hydroperiod and SDC. While the SDC controlled the width of the low saturation zone in the cross-creek direction, the hydroperiod affected the variation of the saturation along the creek – an increase in hydroperiod led to a rise of saturation from the upper marsh area to the main channel with the near-creek low saturation zones slightly narrowed (Figures 6d and e). We tested the following function for relating mean soil water saturation (MSS) to hydroperiod and SDC:

$$\mathrm{MSS}=1-a(1-\mathrm{HP})\exp(-b\mathrm{SDC}^{c}), \tag{5}$$

where a, b and c are fitting coefficients. The rationale of equation (5) is based on an exponential damping of tidal effects with distance from the creek over the exposure period proportional to $(1-\mathrm{HP})$. This is consistent with the groundwater wave propagation in unconfined

aquifers (e.g., *Li et al*. [2000]). The damping influences the pore-water drainage underlying the variations of MSS. Equation (5) is composed of separate variables. Its numerical values are dominated by the distance-dependent exponential damping term and modulated linearly by the hydroperiod. Equation (5) was found to fit the simulation results reasonably well with $R^2 = 0.85$, $a = 0.32$, $b = 1.57$ and $c = 0.39$. This equation predicted essentially the same spatial pattern of mean soil water saturation as simulated numerically (Figure 8).

The behavior of SSI and mean soil water saturation is fundamentally linked to the pore-water flow. The drainage process associated with the tide-induced circulation (net efflux) directly affected the local groundwater table elevation and soil water saturation. We calculated the net water flux across the marsh surface over the semi-diurnal tidal cycle. The net water influx occurred on the marsh platform, accompanied by the net water efflux from the creek bank and bottom, and the main channel bank (Figure 6f). The spatial pattern of the net water flux resembled those of SSI and mean soil water saturation with a correlation coefficient of 0.76 between net water flux and SSI, and 0.94 between net water flux and mean soil water saturation. With this high correlation, the soil aeration represented by SSI and mean soil water saturation was in alignment with the soil flushing represented by net water flux; both conditions are likely to be important for plant growth and distribution as discussed earlier.

Spring-neap tidal simulation

As the tidal regime switched from the monochromatic to spring-neap tides, the hydroperiod in the upper marsh area decreased (Figure 7b vs. Figure 6b). This area was inundated daily and remained nearly saturated over the spring tides. However, it was exposed and be-

came unsaturated to a considerable degree due to cumulative drainage during the neap tides (Figure 4b). Consequently, a zone of relatively low soil water saturation formed in the upper marsh area including the interior, in addition to the near-creek low saturation zones (Figures 7d and 7e). In contrast, the hydroperiod in the lower marsh area increased, resulting in a slight increase of local soil water saturation and narrowing of the near-creek low saturation zone (Figures 7d and 7e). The spatial variations of the SSI and mean soil water saturation also correspond well with each other (correlation coefficient = 0.98).

We also tested equation (5) for the spring-neap tidal case. While the relationship does not apply to the whole marsh system, the test focused on the lower marsh area for $y \leq 160$ m (marsh platform elevation ≤ 6.8 m, below the neap high tide mark), where the inundation occurred at a constant frequency of twice a day (Figure 9a). The result showed that equation (5) described well the mean soil water saturation in this lower marsh area with $R^2 = 0.84$, $a = 0.35$, $b = 1.72$ and $c = 0.36$ (Figure 9b). All fitting parameter values are close to those for the monochromatic case.

In the upper marsh ($y \geq 160$ m), the frequency of local platform inundation decreased with the distance from the main channel (Figure 10), due to the variations of the tidal range over the spring-neap cycle (Figure 2). As it is inundated less frequently, the upper marsh continued to drain to the creek until the next flooding tide. When the subsequent inundation occurred, surface water rapidly infiltrated the soil and raised the local soil water saturation to 100%. To account for the effect of varying inundation frequency on the mean soil water saturation, we modified equation (5), with reduced damping for lower frequency oscillations (pe-

riodic inundation events),

$$\mathrm{MSS}=1-d(1-\mathrm{HP})\exp\left[-e\left(\mathrm{IF}+f\right)\mathrm{SDC}^{g}\right], \tag{6}$$

where IF is the inundation frequency, depending on marsh surface elevation (Figure 10); and d, e, f and g are fitting coefficients. Equation (6) fitted well the variations of simulated mean soil water saturation with $R^2 = 0.94$, $d = 0.10$, $e = 0.05$, $f = -2.92$ and $g = 0.36$ (Figure 9).

The change of the tidal regime, however, did not lead to significant modifications of the net water flux pattern, which is similar to that of the monochromatic case. Although the upper marsh area became drier over the neap tides and the inundation during the subsequent (first) spring high tide led to higher infiltration through the marsh surface, the local net water influx over the whole spring-neap cycle changed little. No increase of the net influx was evident in the upper marsh area where a relatively low saturation zone formed. In other words, the degree of flushing given by net water flux was not fully in line with the soil aeration condition. Consistently, net water flux was no longer correlated with either SSI or mean soil water saturation (correlation coefficient < 0.1).

We next consider how these three conditions (SSI, mean soil water saturation and net water flux) combine to influence the plant growth and distribution. A particular combination based on SSI and net water flux (NWF) was tested as a possible composite index (CI),

$$\mathrm{CI}=\theta(1-\mathrm{SSI})+(1-\theta)\frac{\mathrm{NWF}_{\mathrm{local}}-\mathrm{NWF}_{\mathrm{minimum}}}{\mathrm{NWF}_{\mathrm{maximum}}-\mathrm{NWF}_{\mathrm{minimum}}}, \tag{7}$$

where θ and $(1-\theta)$ are weighting factors applied to the soil aeration and flushing conditions,

respectively; and a normalized net water flux has been used. Physically, the two weighting factors would be related to the dependence of the plant carrying capacity (maximum growth rate) on the soil aeration and flushing conditions, respectively. The calculated CI based on the simulations showed different patterns depending on the weighting factor (Figure 11). Overall, while the two conditions reinforce each other mainly in the near-creek area, the lack of synergy between the two leads to potentially less optimal soil conditions for plant growth in the upper marsh. This composite index is hypothetical and yet to be tested against field data; however, the essence of the combination is that an index of soil conditions relevant for plant growth should take into account the effects of all the factors included in equation (7).

To quantify further the changes within the whole marsh system, we ranked the four indices (hydroperiod, SSI, mean soil water saturation and net water flux) for 28,000 locations uniformly distributed over the marsh surface and calculated the cumulative exceedance percentage (similar to cumulative probability used in statistical analysis). When the tidal regime changed from monochromatic to spring-neap, the hydroperiod decreased over 35% of the marsh area as indicated by the intersection of two lines in Figure 12a. This decrease occurred mainly in the upper marsh area with relatively small hydroperiod values (less than 0.5, Figure 12a) and led to reduction in the overall soil water saturation within the marsh system (Figure 12c). The percentage of marsh area with lower saturation increased at all saturation levels (between 0.97 and 1) as a result of the tidal regime changing from monochromatic to spring-neap (Figure 12c). However, this uniform change (as with mean soil water saturation) did not occur for the SSI (Figure 12b): For SSI > 0.85, the exceedance percentage for the spring-neap tidal case was lower than that for the monochromatic tidal case whereas the op-

posite trend occurred for low-SSI values (< 0.85). As discussed earlier, low SSI values were related to the near-creek zones and high SSI values with the marsh interior (Figure 6d). This cumulative percentage result demonstrated consistently that the spring-neap tides led to improvement of the soil aeration (with reduced SSI) in the marsh interior, particularly in the (high-elevation) upper marsh. In the lower marsh, the soil aeration, however, worsened due to the increase in hydroperiod (HP > 0.6, Figure 12a).

Under the influence of the monochromatic tide, the net effluxes to the creek and main channel were about 19.25 m^3/d and 3.91 m^3/d, respectively. Under the spring-neap tides, the net effluxes decreased to 18.43 m^3/d (to the creek) and 2.64 m^3/d (the main channel). It can be seen from Figure 12d that only about 16% of the total marsh surface area contributed to the net efflux in both cases. This area was made up by the creek bank and bottom, and the main channel bank. The cumulative exceedance percentages of net fluxes appeared to overlap noticeably for the two different tidal regime cases (Figure 12d). We ran additional simulations with different semi-diurnal solar (A_1 = 0.35 m) and semi-diurnal lunar (A_2 = 0.65 m) amplitudes. The cumulative exceedance percentages calculated based the additional simulations differed for the two cases, suggesting that the overlapping evident in Figure 12d was not a general characteristic. Net water flux reflects the interaction between the marsh and coastal sea. A large net water efflux signifies a well-drained system. Even so, the spatial variability of drainage may significantly affect the soil conditions and hence play a key role in plant zonation.

4. Discussions

Tide-induced inundation of marsh platform has a strong effect on the marsh soil conditions [*Morris*, 1995; *Ursino et al*., 2004; *Li et al*., 2005; *Marani et al*., 2006; *Silvestri et al*., 2005; *Moffett et al*., 2010]. However, the hydroperiod index may not represent properly the soil conditions. Surface water infiltrates the soil rapidly as inundation of the marsh platform takes place, in contrast to the slow drainage during exposure [*Ursino et al*., 2004; *Xin et al*., 2009, 2011; *Moffett et al*., 2012]. The simulations presented here show distinct differences in soil water saturation between the daily inundated and less frequently inundated marsh areas. Within the marsh system subjected to the influence of spring-neap tides, relatively well aerated zones form near the creek within a relatively short distance in the lower area where inundation occurs at a constant frequency of twice daily – similar to the effect of a monochromatic tide. This contrasts with the well aerated zones in the upper marsh area that expand increasingly as the inundation frequency decreases. Clearly, the inundation frequency plays a crucial role in determining the soil aeration and should be considered in combination with hydroperiod. Although both parameters are related to the marsh surface elevation relative to the tide, inundation frequency represents the effect of rapid surface water infiltration to the marsh soil whereas hydroperiod, as the complement of exposure period, reflects the influence of slow drainage of pore-water from the marsh soil to the creek. Equations (5) and (6) express the relationship between the mean soil water saturation and local morphological and tidal conditions (represented by shortest distance to creeks, hydroperiod and inundation frequency). These formulas are yet to be validated against field data. In addition, there remains a question whether they apply to systems with more complex morphology, e.g., creek network and mul-

tiple, random marsh surface slopes.

The simulation results show that well aerated and flushed zones co-exist near the creek in the form of narrow strips, under the influence of both monochromatic and spring-neap tides. This is consistent with previous field observations that the well aerated and low-salinity zones co-exist near the creek [*Moffett et al*., 2010; *Cao et al*., 2012]. This feature, however, disappears in the upper area of the marsh subjected to spring-neap tides. While improved soil aeration occurs widely in this area including the marsh interior as a result of continuous drainage during the exposure of local marsh surface over the neap tides, the amount of flushing remains poor especially in the interior. This would possibly lead to a high-salinity zone due to salt accumulation under the influence of evapotranspiration [*Morris*, 1995; *Silvestri et al*., 2005]. In this case, a composite index should be introduced to describe the suitability of the combined soil conditions for plant growth dependent on the relative importance of aeration versus salt stress. Overall, the simulation results suggest that, for a marsh subjected to spring-neap tides, (a) the lower marsh area, with only the very narrow near-creek zones aerated, is likely to be dominated by bare mud flats [*Morris et al*., 2002]; (b) the near-creek zones in the upper marsh may have suitably aerated soil and low salinity pore-water suitable for the development of different plant species; and (c) in the upper inner marsh area, salt-tolerant species may adapt to the local soil with a reasonable aeration state but possibly high salinity. It is important to note that plant growth and zonation depend not only on the eco-system's carrying capacity under particular soil conditions but also on the influence of intra- and inter-species competitions [*Bertness et al*., 1992; *Costa et al*., 2003; *Pennings et al*., 2005]. Therefore, even well determined soil conditions may not be linked simply to observed

plant zonation [*Armstrong et al*., 1985; *Moffett et al*., 2010].

Simulated marsh systems under the influence of monochromatic and spring-neap tides exhibited distinct differences in soil aeration and flushing conditions. These differences are manifested in spatial variations of marsh soil water saturation and net water flux, and are additionally reflected in the statistics of these soil condition parameters in terms of their occurrence probability. For example, the occurrence of relatively low soil water saturation is more probable in the system forced by spring-neap tides. Based on these results, we suggest that future investigations should be designed to explore further the effects of multi-constitute tides on salt marshes.

Morphological and tidal factors, including marsh surface elevation, shortest distance to creeks, hydroperiod and inundation frequency, combine to influence mean soil water saturation, soil saturation index (SSI) and net water flux. For the modeled marsh systems under monochromatic and spring-neap tides, relationships were established to quantify such combined effects, with mean soil water saturation described by a function of morphological and tidal parameters. While this function for the daily flooded marsh area mainly depends on SDC and hydroperiod, the upper marsh in the spring-neap tidal case is significantly affected by inundation frequency. These results extend previous findings from 2-D models on pore-water flow processes and soil conditions in salt marshes. For example, the effects of sea level rise on salt marshes, as shown by *Wilson and Morris* [2012] based on a constant change of hydroperiod along a 2-D cross-creek transect, could be even more severe if the modification of the inundation frequency across a 3-D marsh system is considered.

The present study focused on the tide-induced pore-water flow and associated soil conditions. While the tide is a key driving force for salt marshes, other processes, including precipitation and evapotranspiration also affect water balance and pore-water flow in the marsh soil, particularly within the inner area [*Ursino et al*., 2004; *Silvestri and Marani*, 2004; *Marani et al*., 2006; *Xin et al*., 2011]. The flow may also be influenced by density gradients due to variations of surface water and pore-water salinity (the variable salinity itself would be an important factor for understanding the distribution of salt-tolerant and salt-intolerant plants).

Given uncertainty with marsh morphology and soil heterogeneity as well as random rainfall events and plant species competitions, applications of the modeling results to field sites with typically limited data would be difficult at this stage. Nevertheless, we searched Google Earth for sites with plant distribution patterns that are consistent with our results and found a number of candidate marsh systems. For example, the plant distribution in the Welwick marsh (Figure 13) is affected by spring-neap tides, and appears to exhibit a fan-shaped pattern in the upper area above the creek end in addition to stripes along the creek, consistent with our simulation results (Figure 11). This pattern was linked to measured soil aeration conditions by *Armstrong et al*. [1985].

5. Concluding remarks

Recent numerical studies have examined the suitability of soil conditions for plant growth based on 2-D vertical cross-creek sections. These studies focused on soil aeration in relation to plant respiration and neglected other important soil conditions like nutrient and salt concentrations. Naturally, these models cannot fully represent the 3-D pore-water flow

characteristics and spatial variations of soil conditions. The present study, aiming to overcome these shortcomings, examined six indices in a modeled 3-D creek-marsh subjected to both monochromatic and spring-neap tides. The shortest distance to creeks (SDC) was found to be a critically important factor affecting the soil conditions. Well aerated and drained/flushed zones co-existed near the creek under both monochromatic and spring-neap tides. Spring-neap tides led to improved soil aeration in the upper marsh, including the interior section where the hydroperiod and inundation frequency were reduced during neap tides. This, however, was not accompanied by improved soil flushing.

These findings have implications for investigations of marsh eco-hydrology in relation to plant zonation. Field experiments can be designed to collect measurements aiming to test the modeling results, e.g., the relationship of the mean soil water saturation with SDC, hydroperiod and inundation frequency as described by equations (5) and (6). Such a relationship is a key to unraveling plant zonation in natural marsh eco-systems.

Acknowledgments

This research was supported by the Australian Research Council (DP0988718). P. X. acknowledges an Early Career Researcher Grant provided by The University of Queensland (603275). The authors acknowledge valuable comments from Drs. A. M. Wilson and J. N. King, an anonymous reviewer and the Associate Editor, which led to significant improvement of the paper.

References

Allen, J. R. L. (2000), Morphodynamics of Holocene salt marshes: A review sketch from the Atlantic and Southern North Sea coasts of Europe, *Quaternary Science Reviews*, *19*(12), 1155-1231, doi: 10.1016/S0277-3791(99)00034-7.

Armstrong, W. (1982), Waterlogged soils. In *Environmental Plant Ecology*, 2nd ed., Etherington, J. R., ed. John Wiley: Hoboken, NJ, USA.

Armstrong, W., E. J. Weight, S. Lythe, and T. J. Gaynard (1985), Plant zonation and the effects of the spring-neap tidal cycle on soil aeration in a Humber salt marsh, *Journal of Ecology, 73*, 323-339, doi: 10.2307/2259786.

Armstrong, W., and M. Drew (2002), Root growth and metabolism under oxygen deficiency. In: Waisel E. A., Kafkafi Y., eds. *Plant Roots: The Hidden Half.* Marcel Dekker, New York, NY, USA: pp. 729-761.

Bertness, M. D., L. Gough, and S. W. Shumway (1992), Salt tolerances and the distribution of fugitive salt marsh plants, *Ecology 73*(5), 1842-1851, doi: 10.2307/1940035.

Cao, M., P. Xin, G. Jin, and L. Li (2012), A field study on groundwater dynamics in a salt marsh – Chongming Dongtan wetland, *Ecological Engineering, 40*, 61-69, doi: 10.1016/j.ecoleng.2011.12.018.

Carol, E. S., E. E. Kruse, and J. L. Pousa (2011), Influence of the geologic and geomorphologic characteristics and of crab burrows on the interrelation between surface water and groundwater in an estuarine coastal wetland, *Journal of Hydrology, 403*(3-4) 234-241, doi: 10.1016/j.jhydrol.2011.04.007.

Carsel, R. F., and R. S. Parrish (1988), Developing joint probability distributions of soil water retention characteristics, *Water Resources Research, 24*(5), 755-769, doi: 10.1029/WR024i005p00755.

Chapman, V. J. (1960), *Salt Marshes and Salt Deserts of the World*. Leonard Hill, London, UK.

Chen, X. (1998), Changjiang (Yangtze) River Delta, China, *Journal of Coastal Research, 14*(3), 838-858.

Colmer, T. D., and T. J. Flowers (2008), Flooding tolerance in halophytes, *New Phytologist, 179*(4), 964-974, doi: 10.1111/j.1469-8137.2008.02483.x.

Costa, C. S. B., J. C. Marangoni, and A. M. G. Azevedo (2003), Plant zonation in irregularly flooded salt marshes: relative importance of stress tolerance and biological interactions, *Journal of Ecology*, *91*(6), 951-965, doi: 10.1046/j.1365-2745.2003.00821.x.

Dacey, J. W. H., and B. L. Howes (1984), Water uptake by roots controls water table movement and sediment oxidation in short Spartina marsh, *Science, 224*(4648), 487-489, doi: 10.1126/science.224.4648.487.

Dolphin, T. J., T. M. Hume, and K. E. Parnell (1995), Oceanographic processes and sediment mixing on a sand flat in an enclosed sea, Manukau Harbour, New Zealand, *Marine Geology, 128*(3-4), 169-181, doi: 10.1016/0025-3227(95)00097-I.

Freeze, R. A., and J. A. Cherry (1979), *Groundwater*, Prentice-Hall, Englewood Cliffs, NJ,

USA.

Gardner, L. R. (2005), Role of geomorphic and hydraulic parameters in governing pore water seepage from salt marsh sediments, *Water Resources Research, 41*(7), W07010, doi: 10.1029/2004WR003671.

Gardner, L. R., and D. E. Porter (2001), Stratigraphy and geologic history of a southeastern salt marsh basin, North Inlet, South Carolina, USA, *Wetlands Ecology and Management, 9*(5) 371-385, doi: 10.1023/A:1012060408387.

Gardner, L. R., and A. M. Wilson (2006), Comparison of four numerical models for simulating seepage from salt marsh sediments, *Estuarine, Coastal and Shelf Science, 69*(3-4) 427–437, doi: 10.1016/j.ecss.2006.05.009.

Godin, G. (1972), *The Analysis of Tides*, University of Toronto Press: Toronto, Ontario, Canada.

Harvey, J. W., P. F. Germann, and W. E. Odum (1987), Geomorphological control of subsurface hydrology in the creek bank zone of tidal marshes, *Estuarine, Coastal and Shelf Science*, *25*(6), 677-691, doi: 10.1016/0272-7714(87)90015-1.

Howes, B. L., and D. D. Goehringer (1994), Porewater drainage and dissolved organic carbon and nutrient losses through the intertidal creekbanks of a New England salt marsh, *Marine Ecology Progress Series, 114*(3), 289-301, doi: 10.3354/meps114289.

Howes, B. L., R. W. Howarth, J. M. Teal, and I. Valiela (1981), Oxidation-reduction potentials in a salt marsh: Spatial patterns and interactions with primary production, *Lim-*

nology and Oceanography, 26(2), 350-360.

Hughes, C. E., P. Binning, and G. R. Willgoose (1998), Characterisation of the hydrology of an estuarine wetland, *Journal of Hydrology, 211*(1-4), 34-49, doi: 10.1016/S0022-1694(98)00194-2.

King, J. N., A. J. Mehta, and R. G. Dean (2010), Analytical models for the groundwater tidal prism and associated benthic water flux, *Hydrogeology Journal, 18*(1), 203-215, doi: 10.1007/s10040-009-0519-y.

Li, L., D. A. Barry, F. Stagnitti, J.-Y. Parlange, and D.-S. Jeng (2000), Beach water table fluctuations due to spring-neap tides: Moving boundary effects, *Advances in Water Resources, 23*(8), 817-824, doi.org/10.1016/S0309-1708(00)00017-8.

Li, H. L., L. Li, and D. Lockington (2005), Aeration for plant root respiration in a tidal marsh, *Water Resources Research*, *41*(6)*,* W06023, doi: 10.1029/2004WR003759.

Marani, M., S. Silvestri, E. Belluco, N. Ursino, A. Comerlati, O. Tosatto, and M. Putti (2006), Spatial organization and ecohydrological interactions in oxygen-limited vegetation ecosystems, *Water Resources Research, 42*(6), W06D06, doi: 10.1029/2005WR004582.

McKee, K.L., and W. H. Patrick (1988), The relationship of smooth cordgrass (*Spartina alterniflora*) to tidal datums: A review, *Estuaries and Coasts, 11*(3), 143-151, doi: 10.2307/1351966.

Mendelssohn, I. A., K. L. McKee, and W. H. Patrick (1981), Oxygen deficiency in Spartina

alterniflora roots: Metabolic adaptation to anoxia, *Science, 214*(4519), 439-441, doi: 10.1126/science.214.4519.439.

Moffett, K. B., D. A. Robinson, and S. M. Gorelick (2010), Relationship of salt marsh vegetation zonation to spatial patterns in soil moisture, salinity and topography. *Ecosystems, 13*(8): 1287-1302, doi: 10.1007/s10021-010-9385-7.

Moffett, K. B., S. M. Gorelick, R. G. McLaren, and E. A. Sudicky (2012), Salt marsh ecohydrological zonation due to heterogeneous vegetation - groundwater - surface water interactions, *Water Resources Research*, *48*, W02516, doi: 10.1029/2011WR010874.

Montalto, F. A., T. S. Steenhuis, and J.-Y. Parlange (2006), The hydrology of Piermont Marsh, a reference for tidal marsh restoration in the Hudson river estuary, New York, *Journal of Hydrology, 316*(1-4), 108-128, doi: 10.1016/j.jhydrol.2005.03.043.

Morris, J. T. (1995), The mass balance of salt and water in intertidal sediments: Results from North Inlet, South Carolina, *Estuaries and Coasts*, 18, 556-567, doi: 10.2307/1352376.

Morris, J. T., P. V. Sundareshwar, C. T. Nietch, B. Kjerfve, and D. R. Cahoon (2002), Responses of coastal wetlands to rising sea level, *Ecology, 83*, 2869-2877, doi: 10.2307/3072022.

Novakowski, K. I., R. Torres, L. R. Gardner, and G. Voulgaris (2004), Geomorphic analysis of tidal creek networks, *Water Resources Research, 40*(5), W05401, doi: 10.1029/2003WR002722.

Pennings, S. C., M.-B. Grant, and M. D. Bertness (2005), Plant zonation in low-latitude salt

marshes: Disentangling the roles of flooding, salinity and competition, *Journal of Ecology*, 93, 159-67, doi: 10.1111/j.1365-2745.2004.00959.x.

Perillo, G. M. E., D. R. Minkoff, and M. C. Piccolo (2005), Novel mechanism of stream formation in coastal wetlands by crab–fish–groundwater interaction, *Geo-Marine Letters, 25*(4), 214-220, doi: 10.1007/s00367-005-0209-2.

Reeves, H. W., P. M. Thibodeau, R. G. Underwood, and L. R. Gardner (2000), Incorporation of total stress changes into the groundwater model SUTRA, *Ground Water, 38*(1), 89-98, doi: 10.1111/j.1745-6584.2000.tb00205.x.

Sadro, S., M. Gastil-Buhl, and J. Melack (2007), Characterizing patterns of plant distribution in a southern California salt marsh using remotely sensed topographic and hyperspectral data and local tidal fluctuations, *Remote Sensing of Environment, 110*, 226-239, doi: 10.1016/j.rse.2007.02.024.

Sanderson, E. W., T. C. Foin, and S. L. Ustin (2001), A simple empirical model of salt marsh plant spatial distribution with respect to a tidal channel network. *Ecological Modelling, 139*, 293-307, doi: 10.1016/S0304-3800(01)00253-8.

Schultz, G., and C. Ruppel (2002), Constraints on hydraulic parameters and implications for groundwater flux across the upland-estuary interface, *Journal of Hydrology, 260*, 255-269, doi.org/10.1016/S0022-1694(01)00616-3.

Simonini, P., and S. Cola (2002), Some pore pressure measurements at the marsh of S. Felice in the Venice lagoon, in *Scientific Research and Safeguarding of Venice*, *CORILA Research Program 2001 Results*, Ist. Veneto di Sci. Lett. ed Arti, Venice, Italy.

Silvestri, S., and M. Marani (2004), Salt marsh vegetation and morphology, modelling and

remote sensing observations, in *Ecogeomorphology of Tidal Marshes*, Coastal Estuarine Stud., vol. 59, edited by S. Fagherazzi, M. Marani, and L. Blum, pp. 5-25, AGU, Washington, D.C., USA

Silvestri, S., A. Defina, and M. Marani (2005), Tidal regime, salinity and salt marsh plant zonation, *Estuarine, Coastal and Shelf Science, 62*(1-2), 119-130, doi: 10.1016/j.ecss.2004.08.010.

Torres, R., and R. Styles (2007), Effects of topographic structure on salt marsh currents, *Journal of Geophysical Research, 112*(F2), F02023, doi: 10.1029/2006JF000508.

Thibodeau, P. M., L. R. Gardner, and H. W. Reeves (1998), The role of groundwater flow in controlling the spatial distribution of soil salinity and rooted macrophytes in a southeastern salt marsh, USA, *Mangroves and Salt Marshes, 2*, 1-13, doi: 10.1023/A:1009910712539.

Ursino, N., S. Silvestri, and M. Marani (2004), Subsurface flow and vegetation patterns in tidal environments, *Water Resources Research, 40*(5), W05115, doi: 10.1029/2003WR002702.

van Genuchten, M. Th. (1980), A closed form equation for predicting the hydraulic conductivity of unsaturated soils, *Soil Science Society of America Journal, 44*(5)*,* 892-898.

Vernberg, F. J. (1993), Salt-marsh processes: A review, *Environmental Toxicology and Chemistry, 12,* 2167-2193, doi: 10.1002/etc.5620121203.

Voss, C. I., and A. M. Provost (2008), A model for saturated-unsaturated, variable-density ground-water flow with solute or energy transport, U.S. Geological Survey, Water-Resources Investigations Report 02-4231 (http://water.usgs.gov/nrp/gwsoftware/sutra.html, last accessed 13 November 2012).

Wang, Z., J. Feyen, D. R. Nielsen, and M. Th. van Genuchten (1997), Two phase flow infiltration equations accounting for air entrapment effects, *Water Resources Research, 33*(12), 2759-2767, doi: 10.1029/97WR01708.

Wilson, A. M., and J. T. Morris (2012), The influence of tidal forcing on groundwater flow and nutrient exchange in a salt marsh-dominated estuary, *Biogeochemistry, 10*(1-3), 27-38, doi: 10.1007/s10533-010-9570-y.

Wilson, A. M., and L. R. Gardner (2006), Tidally driven groundwater flow and solute exchange in a marsh: Numerical simulations, *Water Resources Research, 42*(1), W01405, doi: 10.1029/2005WR004302.

Wilson, A. M., W. S. Moore, S. B. Joye, J. L. Anderson, and C. A. Schutte (2011), Storm-driven groundwater flow in a salt marsh, *Water Resources Research*, *47*, W02535, doi: 10.1029/2010WR009496.

Xin, P., G. Jin, L. Li, and D. A. Barry (2009), Effects of crab burrows on pore water flows in salt marshes, *Advances in Water Resources, 32*(3), 439-449, doi: 10.1016/j.advwatres.2008.12.008.

Xin, P., B. Gibbes, L. Li, Z. Song, and D. Lockington (2010), Soil saturation index of salt

marshes subjected to spring-neap tides: A new variable for describing marsh soil aeration condition, *Hydrological Processes, 24*(18), 2564-2577, doi: 10.1002/hyp.7670.

Xin, P., J. Kong, L. Li, and D. A. Barry (2012). Effects of soil stratigraphy on pore-water flow in a creek-marsh system, *Journal of Hydrology*, 475, 175-187, doi: 10.1016/j.jhydrol.2012.09.047.

Xin, P., L.-R. Yuan, L. Li, and D. A. Barry (2011), Tidally driven multiscale pore water flow in a creek-marsh system, *Water Resources Research, 47*, W07534, doi: 10.1029/2010WR010110.

Yuan, L., P. Xin, J. Kong, L. Li, and D. Lockington (2011), A coupled model for simulating surface water and groundwater interactions in coastal wetlands, *Hydrological Processes, 25*(23), 3533-3546, doi: 10.1002/hyp.8079.

Zhang, Y. L., A. M. Baptista, and E. P. Myers (2004), A cross-scale model for 3D baroclinic circulation in estuary-plume-shelf systems: I. Formulation and skill assessment, *Continental Shelf Research, 24*(18), 2187–2214, doi: 10.1016/j.csr.2004.07.021.

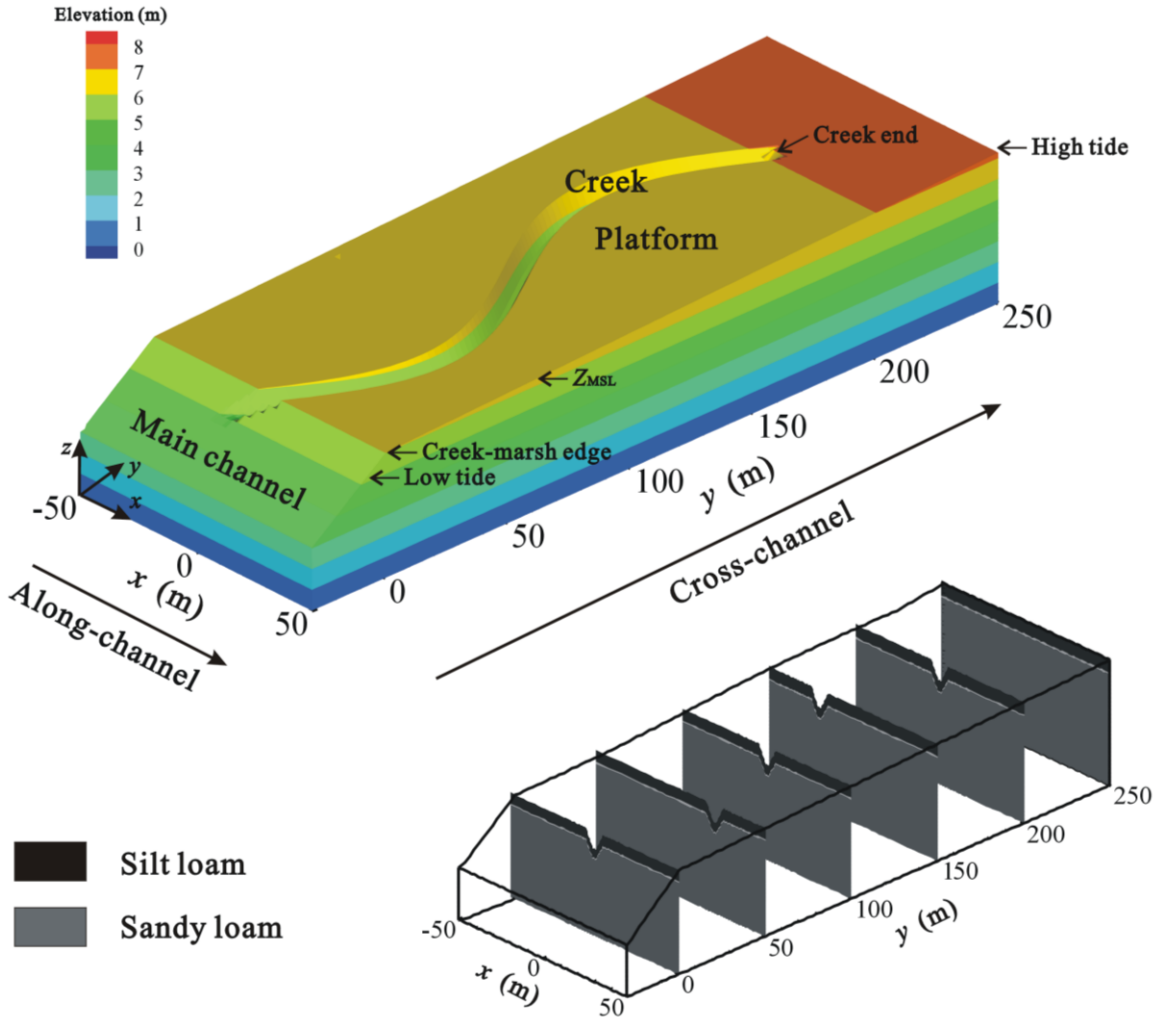

Figure 1. Diagram of the modeled creek-marsh system (after *Xin et al*. [2011]). The contours show the marsh sediment elevation. The scale of the *z* axis is exaggerated by a factor of eight relative to those of the *x* and *y* axes. The soil stratigraphy is illustrated at the lower right corner.

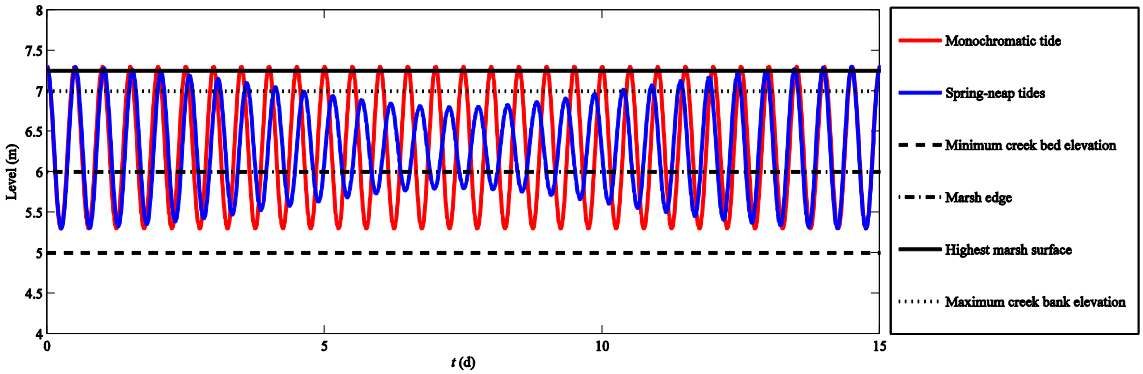

Figure 2. Temporal changes of the tidal water level relative to local marsh surface elevations at various locations.

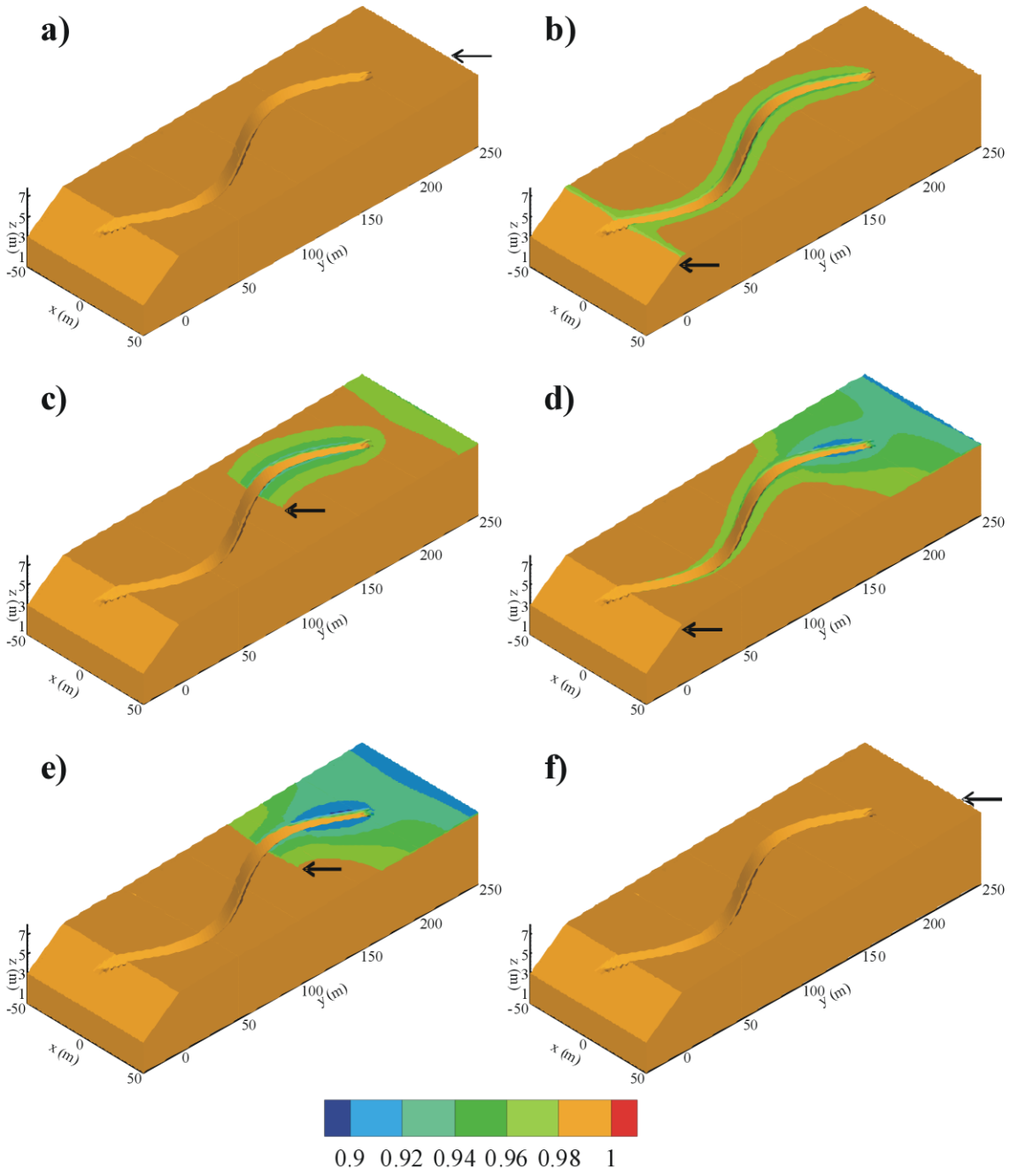

Figure 3. Temporal and spatial variations of soil water saturation at the marsh surface over a spring-neap tidal cycle: (a) spring high tide (7.3 m, elapsed time: 0 d); (b) spring low tide (5.3 m, elapsed time: 0.25 d); (c) neap rising tide (6.61 m, elapsed time: 3.5 d); (d) neap low tide (5.8 m, elapsed time: 7.5 d); (e) neap rising tide (6.68 m, elapsed time: 8.75 d) and (f) spring high tide (7.27 m, elapsed time: 13.47 d). The tidal water levels are indicated by the arrows.

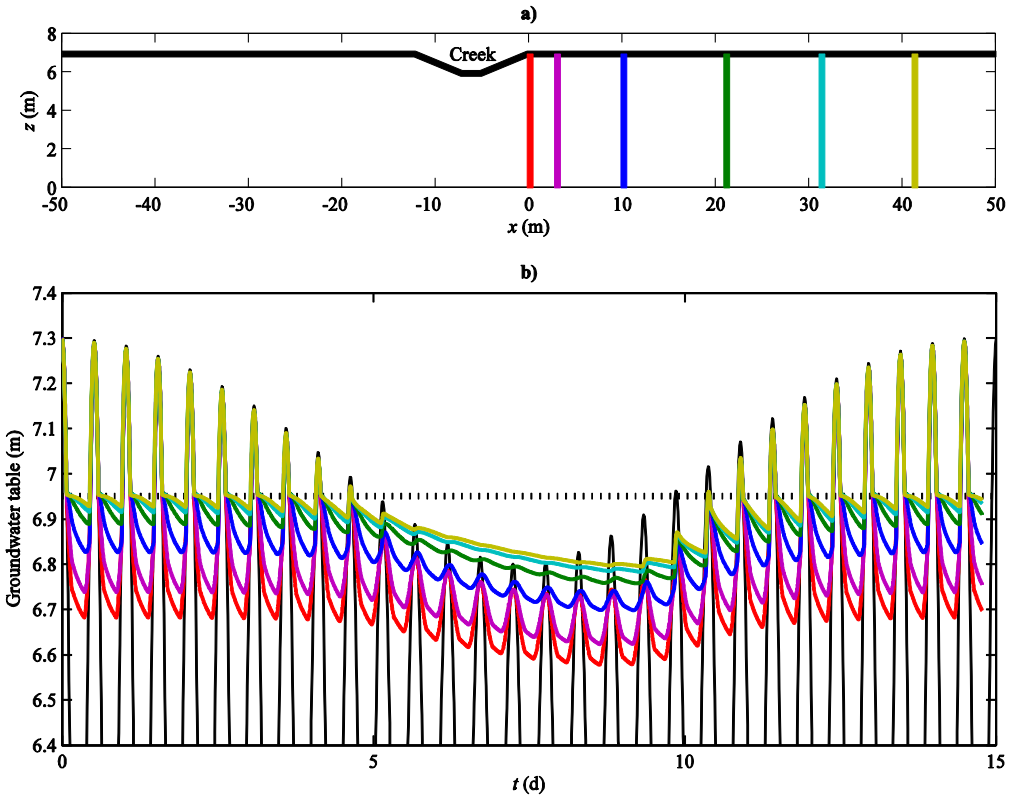

Figure 4. (a) Topography of the cross-creek section along y = 190 m and the six selected locations. (b) Local groundwater table fluctuations. The locations are indicated by the same colors as in (a). The horizontal dotted line indicates the elevation of the local marsh platform (z = 6.95 m). The tidal water level is also plotted (black line).

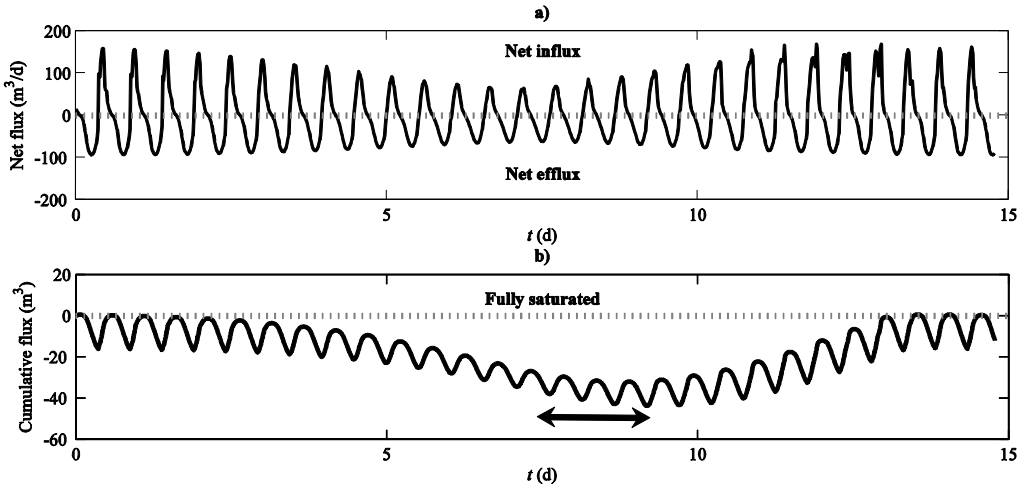

Figure 5. (a) Time-varying net flux across the marsh surface over the whole marsh system and (b) cumulative flux (change in volume of water stored in the marsh soil), which shows the drainage condition in the marsh soil across the whole marsh system. A fully saturated soil condition is given by 0, and negative values indicate partially saturated soil conditions. The arrow indicates the time lag between the minimum cumulative flux and the minimum tidal range at the neap tide.

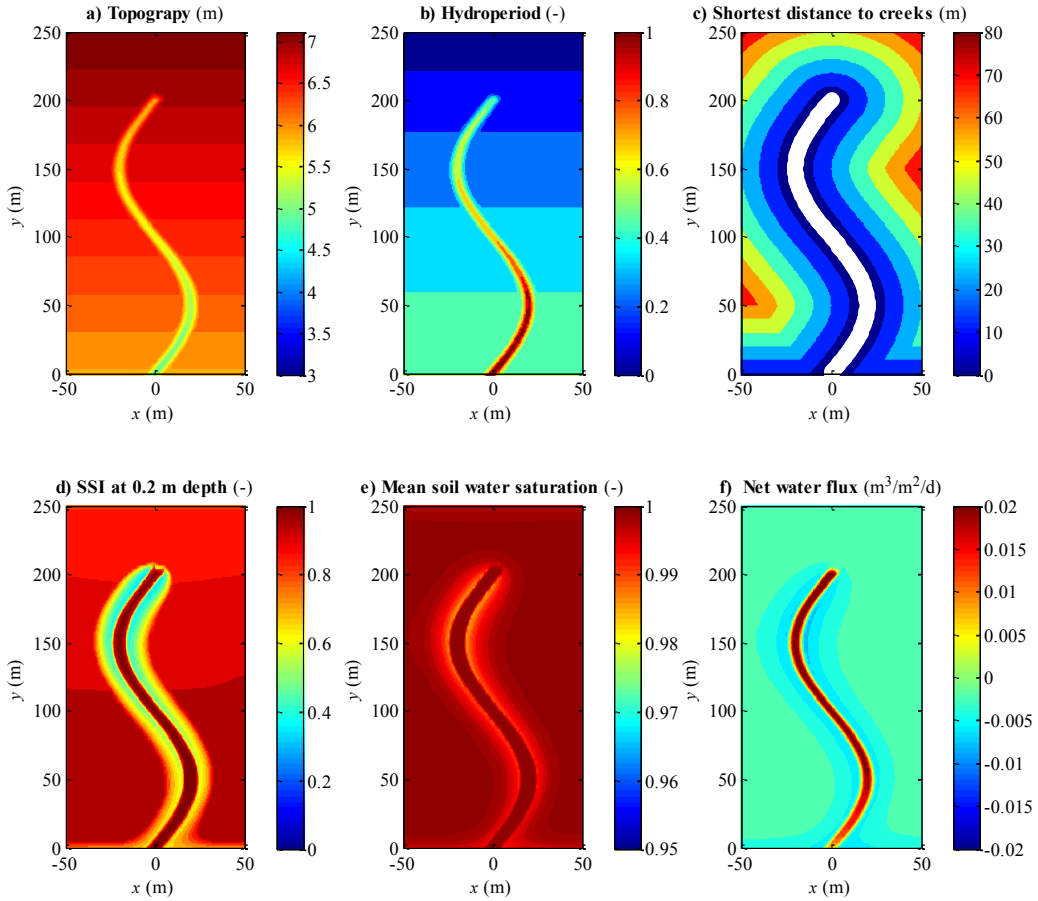

Figure 6. Different indices (shown in the plot titles) calculated over a monochromatic tidal cycle. The reference soil depth is set to 0.2 m.

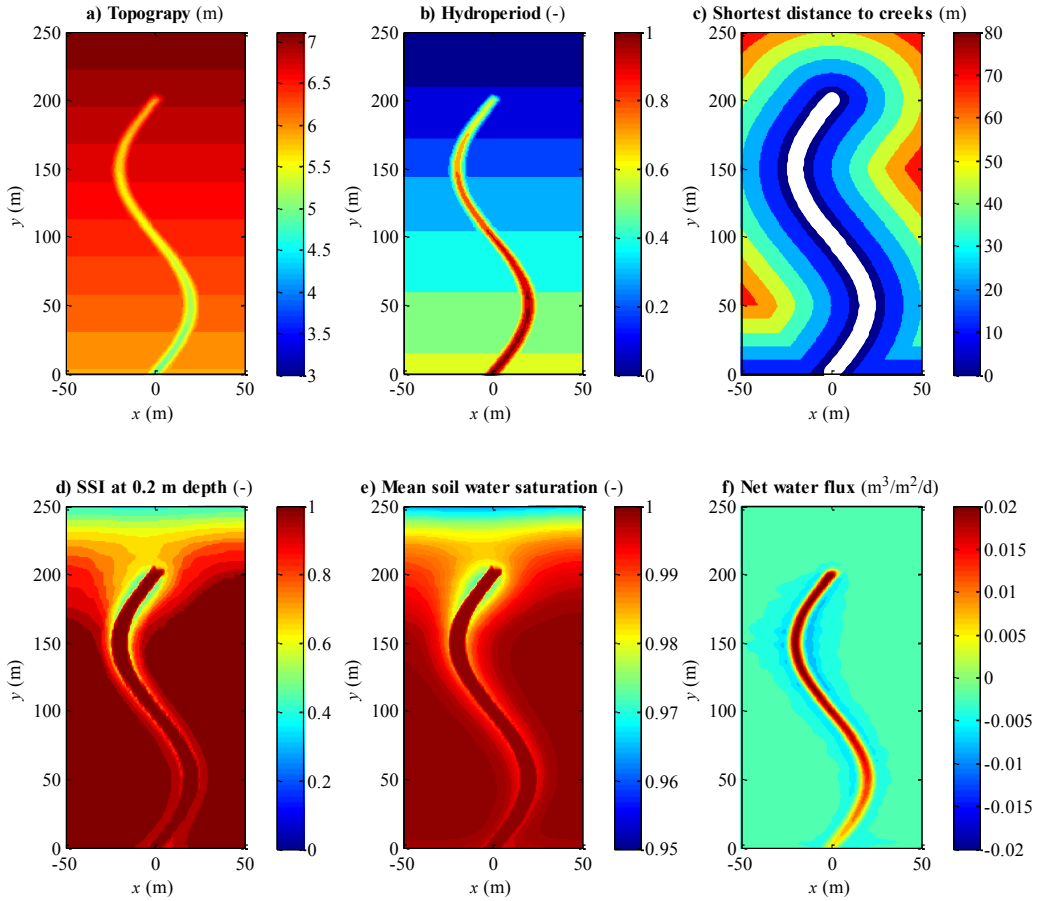

Figure 7. Different indices (shown in the plot titles) calculated over a spring-neap tidal cycle. The reference soil depth is set to 0.2 m.

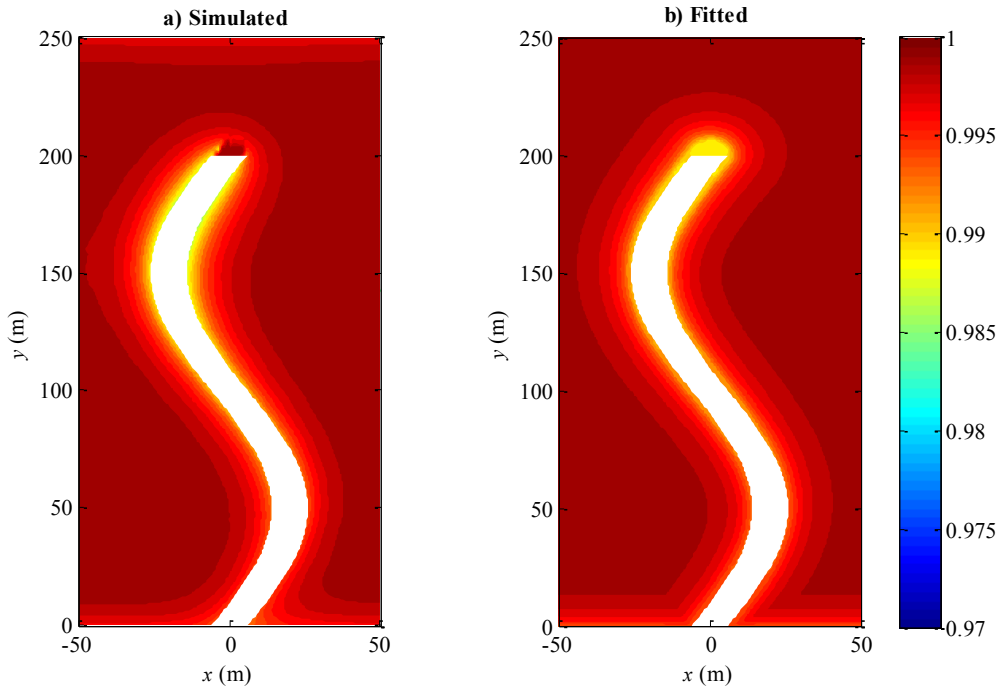

Figure 8. Comparison between the simulated and fitted (based on equation (5)) mean soil water saturation. Results are for the monochromatic tide (Case 1).

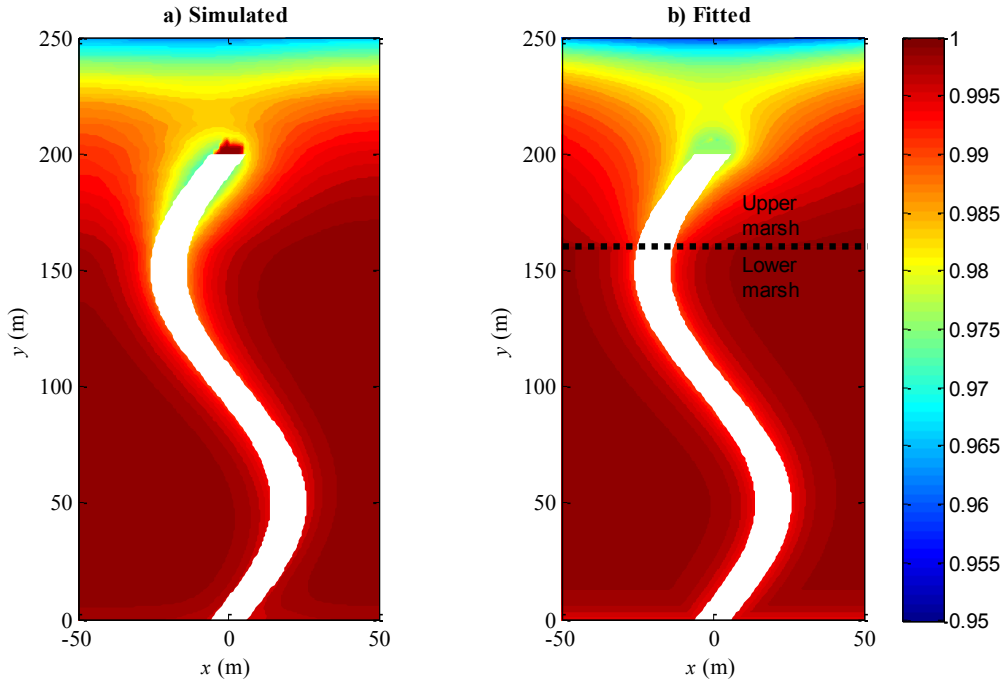

Figure 9. Comparison between the simulated and fitted mean soil water saturation. The lower marsh is fitted based on equation (5) and the upper marsh is fitted based on equation (6). Results are for the spring-neap tides (Case 2).

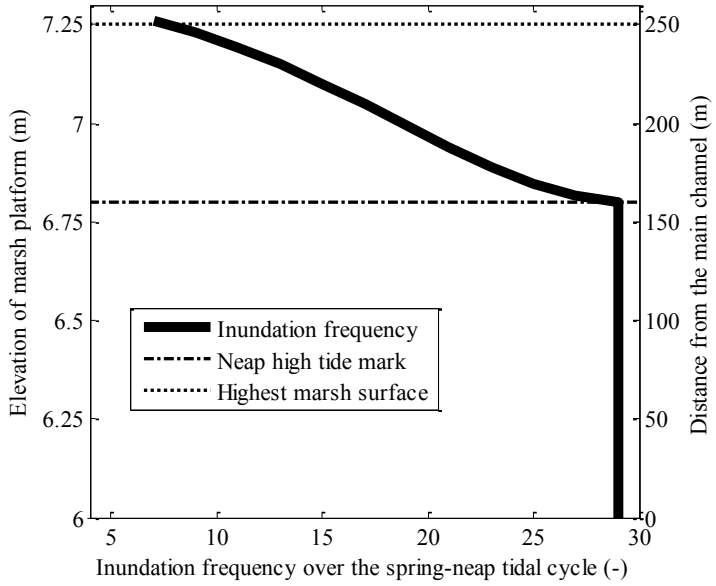

Figure 10. Inundation frequency in terms of numbers of inundation events per spring-neap tidal cycle.

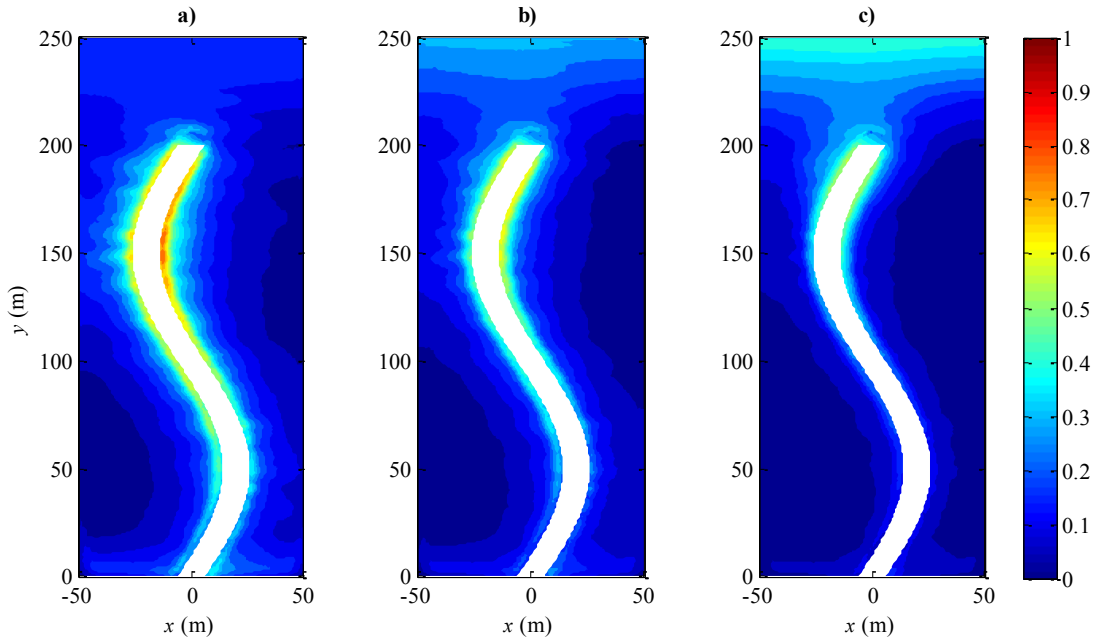

Figure 11. Distribution of the composite index based on the soil saturation index and net water flux (equation (7)). (a) $\theta = 0.25$; (b) $\theta = 0.5$ and (c) $\theta = 0.75$.

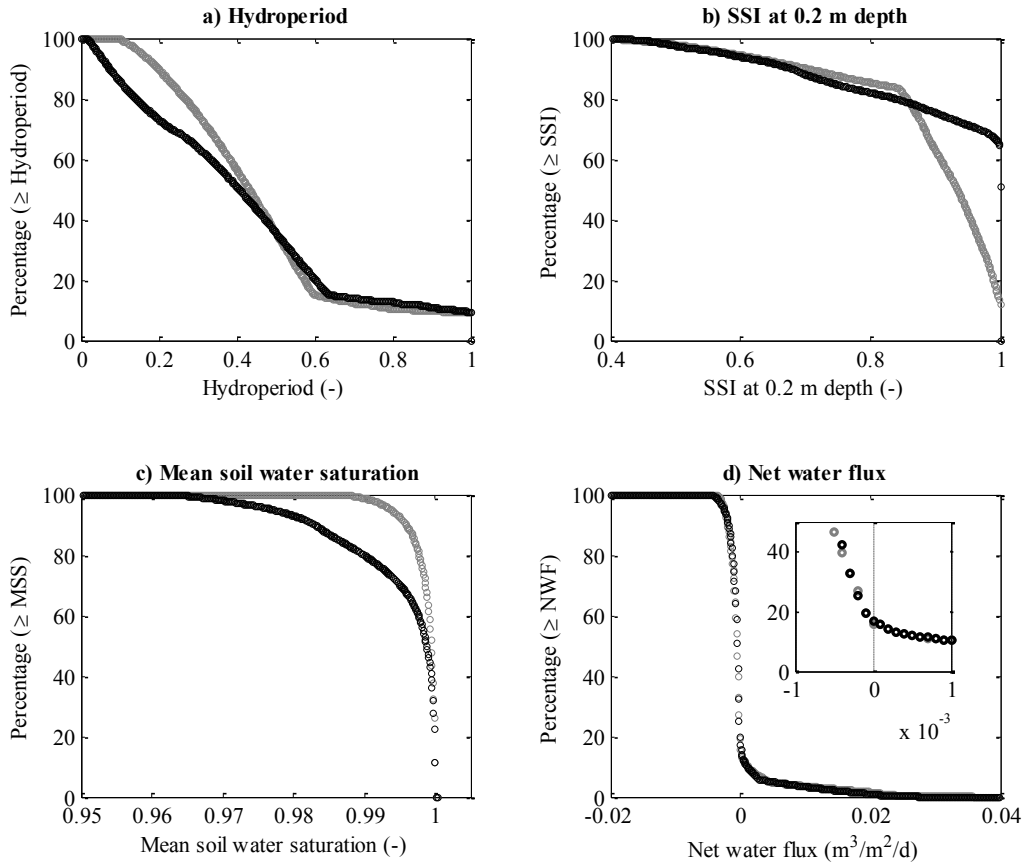

Figure 12. Cumulative exceedance percentage of different indices in the creek-marsh system. The gray circles are for the monochromatic tide and the black circles are for the spring-neap tides. For (d), an enlarged image is also given.

Figure 13. Plant distribution patterns in the Welwick marsh, Yorkshire, England (53°38′57″ N, 0°01′13″ E). The image is from Google Earth (on 24 October, 2012).